

# GENERAL MAGNETIC FIELD OF THE SUN AS A STAR AS INDICATOR OF MASSIVE STREAMS FLOWING ON THE SUN

S. Plachinda<sup>1</sup>, D. Baklanova<sup>1</sup>, I. Han<sup>2</sup>, K.-M. Kim<sup>2</sup>, P. Reegen<sup>3</sup>,  
G. Valyavin<sup>2</sup>, W. Weiss<sup>3</sup>

<sup>1</sup> Crimean Astrophysical Observatory, Nauchny, Crimea, 98409, Ukraine

<sup>2</sup> Korea Astronomy and Space Science Institute, 36-1 Whaam-dong, Yuseong, Daejeon, Korea 305-348

<sup>3</sup> Institut für Astronomie, Turken-schanzstrasse 17, 1180 Vienna, Austria

**ABSTRACT.** The behaviour of the General Magnetic Field of the Sun as a Star (GMFSS) is characterized by the change of amplitude of oscillations with the eleven-year cycle of activity. In maximum of activity GMFSS reaches its maximal values, and in a minimum reaches minimal values. The values of active frequencies vary from cycle to cycle of sunspots activity. Each peak of GMFSS power spectrum is widened by the number of active frequencies. From observations of GMFSS the velocity of solar photosphere movements deviates from the speed of the differential rotation of the Sun more than  $5 \text{ ms}^{-1}$  as it follows from helioseismology. For 40 years of direct observations (two solar magnetic cycles) resulting magnetic field of GMFSS is non equal to zero. GMFSS demonstrates properties of a real large-scale field because there is a balance of positive and negative magnetic fluxes, i.e. the magnetic tubes are closed.

**Key words:** Sun: magnetic fields

## 1. Introduction

The first results of the magnetic field measurements of the Sun as a star were published by Severny (1969). It is the General Magnetic Field of the Sun as a Star (GMFSS). The General Magnetic Field (GMF) is averaged value of the longitudinal component of magnetic structures and weighted by stellar surface brightness distribution. Observations of the Sun's GMF were obtained mainly at four observatories: Crimean Astrophysical Observatory (CrAO), since 1968 on the present time; Mount Wilson Observatory (MWO), since 1970 until 1982; Wilcox Solar Observatory of Stanford University (WSO), since 1975 on the present time (see Solar Geophysical Data); and the Sayan Observatory (Russia), since 1982 on the present time. GMF as the large-scale magnetic field is absent in the Babcock and Leighton phenomenological

magneto-kinematic model of the solar cycle and in terms of standard  $\alpha - \Omega$  dynamo theory. There are only two main components of large-scale magnetic field on the Sun: toroidal magnetic field and axisymmetric poloidal field. Both toroidal (strong) and poloidal (weak) fields change its polarity with the period of 22 ys.

The main properties of GMFSS are:

1. The strength of GMF versus rotational period shows both sign and shape variations. Both dipole, as dominant, and quadrupole components of the field are detected in the observations.
- 2). The amplitude of variations of GMF varies with the period of sunspots cycle: GMF is strongest during peaks in spot activity, reaching values of about 1 - 2 G (see Fig. 1).
- 3). During four decades of direct observations, for mean GMFSS excess of the positive magnetic flux is concentrated on the one side of the Sun, and excess of the negative flux is concentrated on the opposite side (Plachinda and Tarasova, 2000; Haneychuk et al., 2003). Therefore, GMF of the Sun as a star not reverses its polarity with the 22 yr of the solar cycle period.
- 4). The ratio of the positive to negative magnetic flux of GMF  $\Delta_+/\Delta_- \sim 1.0$  in agreement with Maxwell equation  $\vec{\nabla} \cdot \vec{B} = 0$  (the tubes of the induction  $\vec{B}$  are closed in the atmosphere of the Sun) (Plachinda & Tarasova, 2000; Plachinda et al., 2008).

What do we know about GMF on solar-like stars?

The presence of weak GMF (up to some dozen Gauss) for 21 convective stars (F9-M3 spectral types and I-V luminosity classes) is detected (Plachinda, 2004a). For two solar-like stars variations of GMF as a function of the stellar rotation has been determined for more active and more young star than the Sun  $\xi$  Boo A (G8 V) with  $P_{rot} \sim 6.2$  days, and for old solar-like star 61 Cyg A (K5 V) with  $P_{rot} \sim 36.6$  days

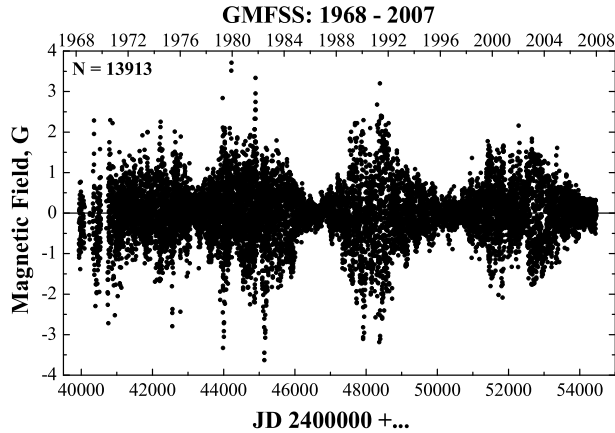


Figure 1: Scatter-plot diagrams for individual GMFSS measurements during the last 40 years. Picture represents combined data for three observatories - CrAO, MWO and WSO. CrAO and MWO data were normalized to WSO data (Kotov et al., 1998).

(Plachinda & Tarasova, 2000; Plachinda, 2004b; Petit et al., 2005).

What the nature of GMFSS phenomenon?

1. The first point of view: we measure magnetic disequilibrium of the Sun. (Haneychuk et al., 2003).
  2. Plachinda & Tarasova (2000) have come to a conclusion that GMFSS together with known toroidal and poloidal fields can be the third large-scale component of a magnetic field of the Sun formed as a result of penetration on a surface of a global magnetic field from a radiative zone.
  3. Livshits & Obridko (2006), analyzing the time series of GMFSS and surface magnetograms of the Sun, have come to a conclusion that GMFSS it is a product of a dynamo mechanism operations.
- This article presents some aspects of the frequency analysis of GMFSS with using softwares ‘SigCpec’ (Reegen, 2007) and ‘Period04’ (Lenz, & Breger, 2005).

## 2. General magnetic field of the Sun as a star

As it was above mentioned the amplitude of GMFSS varies with the eleven year sunspots cycle. In addition, in the upper layers of the Sun the differential rotation and torsion fluctuations of the solar plasma are present. Furthermore, the picture of the distribution of the velocities of torsional oscillations depends on the phase of the cycle of the activity (Howe et al., 2004).

Therefore, due to the frozenness of the magnetic field lines into the plasma, the obtained measurements of the GMFSS must include modulation by the differential rotation, whose rate depends on latitude and falls to the pole of rotation, and to contain modulation as a result of existence of torsional oscillations, i.e., to

contain modulation by surface flows with the different speed of the motion of plasma relative to the smooth curve of differential rotation. From the aforesaid it follows that the observed variability of GMFSS must be described by the large set of active frequencies.

We calculated power spectrum of the all Stanford data ( $N = 9664$  dates during the last 33 years) for the wide frequency range using software SigSpec (Reegen, 2007). In the range of periods (synodic) from 25.7 to 30.8 days the observed picture of GMFSS variability is satisfactorily described by beating the collection of 50 frequencies the alarm probability of which does not exceed  $10^{-5}$  (see Fig. 2).

In Fig. 3 we show the region of the power spectrum with highest peak, which corresponds to the Sun’s rotation with a value at  $26.88596 \pm 0.00086$  days. The half-width of peak (0.0759 days) by two orders exceeds the period error (0.00086 days) as this is marked in the figure. It is obvious that the series of observations GMFSS contains the large number of active frequencies, and each of the peaks is composite and is widened by the collection of frequencies.

The values of active frequencies of prominent peaks of power spectrum significantly vary from the cycle to the cycle of activity. Thus, for the cycle of activity since 1975 until 1986, which is overlapped by Stanford observations, for two most powerful peaks in the spectrum of power  $P_{prim} = 26.8715 \pm 0.0022$  and  $P_{sec} = 27.0800 \pm 0.0027$  days, for the observations of the cycle of the activity since 1987 until 1997  $P_{prim} = 26.9169 \pm 0.0025$  and  $P_{sec} = 27.1426 \pm 0.0031$  days, and for the observations of the cycle of the activity since 1998 until 2008  $P_{prim} = 26.5770 \pm 0.0030$  and  $P_{sec} = 27.1888 \pm 0.0027$  days.

Fig. 4 demonstrates the decrease of the value of periods calculated according to the GMFSS observations with respect to the smooth fitting curve of differential rotation. In this figure the closed marks show the synodic (triangles) and sidereal (circles) periods of the maximum peaks of the power spectrum under conditional envelope, which was carried out on the tops of peaks in the selected frequency range (see Fig. 3). Dashed line and open triangles are helioseismology periods of the differential rotation of the Sun surface in synodic reference frame (left Y axis, sun latitudes). Solid line and closed triangles are magnetic field periods in synodic reference frame (right Y axis, power spectrum amplitudes). Dashed line and open circles are helioseismology periods of the differential rotation of the Sun surface in sidereal reference frame (left Y axis). Solid line and closed circles are magnetic field periods in sidereal reference frame (right Y axis). The above mentioned facts convince us that:

first, *both the differential rotation of the Sun and torsion fluctuations as well as the dependence of behavior GMFSS and torsion fluctuations on the phase of solar activity actually makes the picture of*

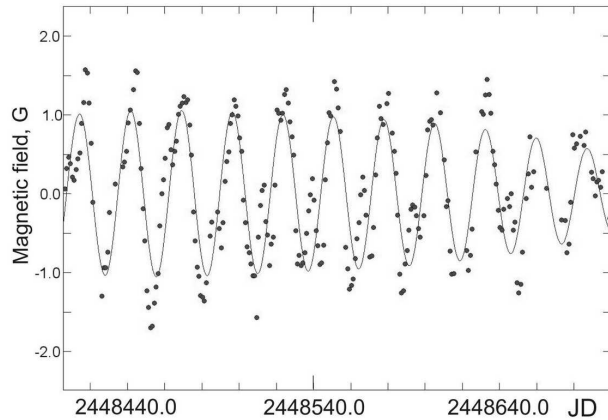


Figure 2: Example of GMFSS behavior in the maximum of solar activity.

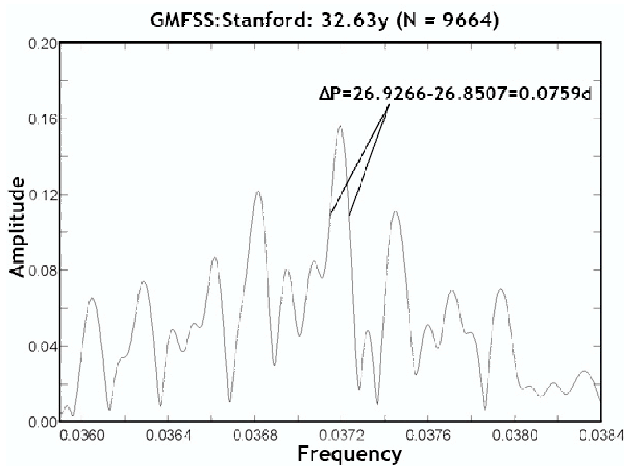


Figure 3: Power spectra.

the behavior GMFSS of complex;

second, an additional shortward displacement between the observed and calculated periods for the smooth curve of differential rotation is presented.

The expected shift between the observed periods and those calculated for the smooth curve of differential rotation, according to the data of helioseismology, must be  $\sim 5 \text{ ms}^{-1}$ . This corresponds to the difference in the periods of  $\sim 0.1$  days for the solar equator. One can see from Fig. 4 that the difference between the obtained periods and expected values noticeably greater than 0.1 days. I.e., in the case of GMFSS observations we record additional to the differential rotation speed of plasma motions in the photosphere of the Sun large than  $5 \text{ ms}^{-1}$ .

*Acknowledgements.* D. Baklanova and S. Plachinda acknowledge support from the Ukrainian Fundamental Research State Fund (M/364); S.Plachinda acknowledges support in part from the Austrian Science Fund (P17890).

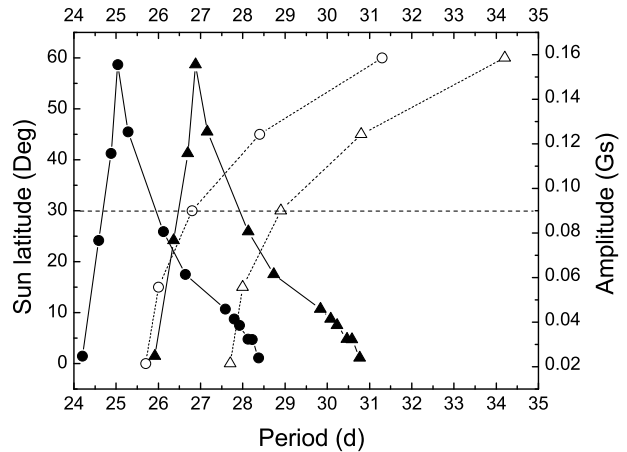


Figure 4: Period diagram

## References

- Haneychuk V.I., Kotov V.A., Tsap T.T.: 2003, *A&Ap*, **403**, 1115.
- Howe R., Komm R.W., Hill F., Christensen Dalsgaard J., Haber D.A., Schou J., Thompson M.J.: 2004, in: *Proc. of the SOHO 14/GONG 2004 Workshop "Helio- and Asteroseismology: Towards a Golden Future"*, ESA SP-559, 472.
- Kotov V.A., Scherrer P.H., Howard R.F., Haneychuk V.I.: 1998, *ApJSS*, **116**, 103.
- Lenz P., Breger M.: 2005, *Comm. in Asteroseismology*, **146**, 53.
- Livshits I.M., Obridko V.N.: 2006, *AstRep*, **50**, N11, 926.
- Petit P., Donati J.-F., Auriere M., Landstreet J.D., Lignieres F., Marsden S., Mouillet D., Paletou F., Toque N., Wade G.A.: 2005, *MNRAS*, **361**, 837.
- Plachinda S.: 2004a, *NATO Science Series*, **161**, 351.
- Plachinda S.: 2004b, in: *Multi-Wavelength Investigations of Solar Activity*, *IAU Symp.*, **223**, 689.
- Plachinda S.I., Tarasova T.N.: 2000, *ApJ*, **533**, 1016.
- Plachinda S., Baklanova D., Han I., Kim K.-M., Reegen P., Valyavin G., Weiss W.: 2008, *BCrAO*, in press.
- Reegen P.: 2007, *A&Ap*, **467**, 1353.
- Severny A.B.: 1969, *Nature*, **224**, 53.